

# Sequential Modification of NEMO/IKK $\gamma$ by SUMO-1 and Ubiquitin Mediates NF- $\kappa$ B Activation by Genotoxic Stress

Tony T. Huang,<sup>1,2</sup> Shelly M. Wuerzberger-Davis,<sup>1,3</sup> Zhao-Hui Wu,<sup>1</sup> and Shigeki Miyamoto<sup>1,2,3,\*</sup>

<sup>1</sup>Department of Pharmacology

<sup>2</sup>Program in Molecular and Cellular Biology

<sup>3</sup>Program in Cancer Biology

University of Wisconsin-Madison

301 SMI

1300 University Avenue

Madison, Wisconsin 53706

## Summary

The transcription factor NF- $\kappa$ B is critical for setting the cellular sensitivities to apoptotic stimuli, including DNA damaging anticancer agents. Central to NF- $\kappa$ B signaling pathways is NEMO/IKK $\gamma$ , the regulatory subunit of the cytoplasmic I $\kappa$ B kinase (IKK) complex. While NF- $\kappa$ B activation by genotoxic stress provides an attractive paradigm for nuclear-to-cytoplasmic signaling pathways, the mechanism by which nuclear DNA damage modulates NEMO to activate cytoplasmic IKK remains unknown. Here, we show that genotoxic stress causes nuclear localization of IKK-unbound NEMO via site-specific SUMO-1 attachment. Surprisingly, this sumoylation step is ATM-independent, but nuclear localization allows subsequent ATM-dependent ubiquitylation of NEMO to ultimately activate IKK in the cytoplasm. Thus, genotoxic stress induces two independent signaling pathways, SUMO-1 modification and ATM activation, which work in concert to sequentially cause nuclear targeting and ubiquitylation of free NEMO to permit the NF- $\kappa$ B survival pathway. These SUMO and ubiquitin modification pathways may serve as anticancer drug targets.

## Introduction

Activation of signal transduction pathways by extracellular stimuli is frequently initiated by the interaction of specific ligands with their cognate cell surface receptors. A variety of mechanisms have been found to transmit these interactions through the cytoplasm into the nucleus to alter the gene expression program via the activation of preexisting transcription factors (Hunter, 2000; Karin and Hunter, 1995). However, very little is known regarding signaling pathways that are initiated in the nucleus and transferred to the cytoplasm—the “nuclear-to-cytoplasmic” signaling pathways.

The NF- $\kappa$ B/Rel family of transcription factors has been intensively studied as an important model system for how extracellular stimuli, such as tumor necrosis factor  $\alpha$  (TNF $\alpha$ ), interleukin-1, or bacterial endotoxin (LPS), cause the activation of latent transcription factors via signal transduction cascades. NF- $\kappa$ B regulates the expression of genes critical for multiple biological processes,

including inflammatory reactions, immune responses, and apoptosis (Ghosh and Karin, 2002; Li and Verma, 2002). NF- $\kappa$ B is normally kept inactive in the cytoplasm of unstimulated cells by its inhibitor proteins, such as I $\kappa$ B $\alpha$  and I $\kappa$ B $\beta$ . Consequently, the release of NF- $\kappa$ B from the I $\kappa$ B proteins is a prerequisite for NF- $\kappa$ B translocation into the nucleus to regulate gene transcription. Interestingly, inactive NF- $\kappa$ B proteins associated with I $\kappa$ B $\alpha$  shuttle between the cytoplasm and the nucleus, but I $\kappa$ B $\beta$  cytoplasmically sequesters inactive NF- $\kappa$ B without nucleocytoplasmic shuttling (Huang and Miyamoto, 2001; Malek et al., 2001; Tam and Sen, 2001). Nevertheless, enucleation experiments have demonstrated that the release of active NF- $\kappa$ B by extracellular stimuli can be accomplished solely within the cytoplasm (Baeuerle and Baltimore, 1988; Devary et al., 1992; Huang et al., 2000b). In contrast, nuclear events are required for activation of NF- $\kappa$ B by certain genotoxic agents (Huang et al., 2000a). Therefore, DNA damage-dependent activation of NF- $\kappa$ B serves as an attractive paradigm to study molecular mechanisms involved in nuclear-to-cytoplasmic signal transduction pathways.

Central to the activation of NF- $\kappa$ B by extracellular stimuli is the I $\kappa$ B kinase (IKK) complex that is composed of two catalytic subunits IKK $\alpha$ /1 and IKK $\beta$ /2, and a regulatory subunit NF- $\kappa$ B essential modulator (NEMO/IKK $\gamma$ ) (Ghosh and Karin, 2002). Signaling pathways converge onto and activate the IKK complex, leading to site-specific phosphorylation of I $\kappa$ B and its degradation by the ubiquitin-proteasome pathway allowing liberation of NF- $\kappa$ B. While transient overexpression of the catalytic subunits alone is sufficient to activate NF- $\kappa$ B, their physiological activation requires the presence of NEMO in the complex. The importance of NEMO in the regulation of IKK and NF- $\kappa$ B activity has been demonstrated in a NEMO-deficient mouse 1.3E2 pre-B cell model and mouse knockout experiments, in which the complete loss of NF- $\kappa$ B activation is shown by various stimuli despite the presence of the catalytic subunits (Li and Verma, 2002). Moreover, two types of human disorders have been genetically linked to mutations occurring in the NEMO gene. Non-sense mutations in the NEMO gene are associated with incontinentia pigmenti (Smahi et al., 2000), whereas point mutations in the encoded C-terminal zinc finger (ZF) domain affecting only a subset of NF- $\kappa$ B activation pathways are found in patients with anhidrotic ectodermal dysplasia in conjunction with immunodeficiency syndromes (Doffinger et al., 2001; Jain et al., 2001). Since NEMO is predicted to be composed of multiple distinct domains (Ghosh and Karin, 2002), these different modules may serve as a signal integrating platform to link a wide range of NF- $\kappa$ B inducing signals to the activation of the IKK catalytic subunits. NEMO was shown to recruit IKK to the T cell receptor (Weil et al., 2003) and the Tax protein of the HTLV-1 directly interacts with NEMO to activate IKK and NF- $\kappa$ B (Sun and Ballard, 1999). The use of a NEMO binding domain (NBD) peptide derived from IKK also indicated that the association between the catalytic subunits and NEMO may not be static in vivo (May et al., 2000). How-

\*Correspondence: smiyamot@wisc.edu

ever, the significance of IKK-NEMO association and dissociation in signal-induced activation of IKK remains unclear.

Like the membrane receptor signaling pathways, those initiated by DNA damaging agents also require NEMO to activate IKK and NF- $\kappa$ B (Huang et al., 2000a; Li and Karin, 1998). Moreover, the ZF domain is essential for DNA damage activation of NF- $\kappa$ B, but it is largely dispensable for LPS signaling (Huang et al., 2002). Mutations that disrupt the ZF were also shown to affect certain types of TNF $\alpha$  receptor superfamily signaling pathways (Jain et al., 2001; Makris et al., 2002). It is possible that the ZF may recruit IKK to the upstream signaling components induced by DNA damage or it may regulate specific NEMO modifications to permit IKK activation. However, the mechanistic role of the NEMO ZF in the NF- $\kappa$ B genotoxic stress pathway is currently unknown.

Posttranslational modification of proteins by the small ubiquitin-like modifier (SUMO) emerged as an important regulatory mechanism (Muller et al., 2001; Pickart, 2001). Presently, there are two models describing the general functions of SUMO modification; it may alter protein stability by competing with ubiquitylation (Desterro et al., 1998) or modulate protein-protein interactions to alter subcellular localization (Mahajan et al., 1997; Matunis et al., 1996; Muller et al., 1998). Although the Ran GTPase-activating protein (RanGAP1), a component of the nuclear import machinery, was the first described SUMO substrate (Mahajan et al., 1997; Matunis et al., 1996), it remains one of few cytosolic substrates of SUMO. Most sumoylated proteins are nuclear (Muller et al., 2001; Seeler and Dejean, 2003). Moreover, SUMO-1 activating and conjugating enzymes are also found predominantly in the nucleus (Rodriguez et al., 2001). A recent study has linked SUMO-1 modification of proliferating cell nuclear antigen (PCNA) as a component of a cellular decision between DNA replication and postreplicative DNA repair following DNA damage induction (Hoegge et al., 2002).

Ataxia telangiectasia mutant (ATM) protein is a critical signal-transducing kinase for mediating certain forms of DNA damage (Abraham, 2001; Kastan and Lim, 2000). DNA double-strand breaks (DSBs) induced by radiation or certain anticancer agents, such as topoisomerase I inhibitor camptothecin (CPT) and topoisomerase II inhibitor etoposide (VP16), have been shown to activate ATM. While the mechanisms involved in ATM activation are beginning to be elucidated (Bakkenist and Kastan, 2003), there are many molecular players that mediate ATM-dependent cell cycle checkpoint and DNA repair regulations. These include CHK1 and CHK2 kinases, BRCA1, NBS1, and p53, among others (Kastan and Lim, 2000; Zhou and Elledge, 2000). ATM has also been implicated in the regulation of DNA damage activation of NF- $\kappa$ B (Li et al., 2001). It is entirely unknown, however, how the principally nuclear ATM kinase causes the activation of the cytoplasmic IKK complex to mediate NF- $\kappa$ B activation.

In the present study, we have examined the role of the NEMO ZF domain in the regulation of IKK activation by genotoxic stress. We provide evidence that these stresses cause nuclear translocation of free NEMO via site-specific SUMO-1 modification in a ZF-dependent manner. We provide further evidence that nuclear localization of NEMO is required to permit subsequent ATM-

dependent ubiquitylation of NEMO. Since IKK activated by DNA damaging agents is ultimately present in the cytoplasm in association with NEMO, our findings suggest that NEMO nuclear transition and modification that are coordinated by SUMO-1 and ATM permit the NF- $\kappa$ B genotoxic stress pathway.

## Results

### DNA Damaging Agents Cause SUMO-1

#### Modification of NEMO in a ZF-Dependent Manner

We previously identified the C-terminal ZF of NEMO to be essential for NF- $\kappa$ B activation by VP16 and CPT (Huang et al., 2002). To probe into the role of this domain, we looked for modifications of NEMO that were induced in a ZF-dependent fashion. Stimulation of NEMO-deficient 1.3E2 cells stably reconstituted with Myc-epitope tagged wild-type (WT) NEMO protein at physiological levels (Huang et al., 2002) with VP16 caused the appearance of a slower migrating band that could only be revealed when cell extracts were prepared by immediately boiling cell suspensions in 1% SDS (Figure 1A). Protein modifications with an increase of  $\sim$ 20 kDa can be associated with SUMO conjugation (Mahajan et al., 1997; Matunis et al., 1996). This protein band was detected by antibodies against Myc-NEMO and SUMO-1 following denaturation and immunoprecipitation (Figure 1A, top images). Thus, it represented covalently SUMO-1 conjugated NEMO. When similarly expressed ZF mutant C417R NEMO was analyzed, we failed to detect any sumoylation (Figure 1A, top images). Thus, intact ZF was required for this SUMO-1 conjugation. VP16-induced sumoylation of NEMO was also seen in HEK293 cells (Figure 1B, lanes 3–5), demonstrating that it was not a 1.3E2 cell line specific event. SUMO-1 modification of NEMO was also evident with CPT, but not with TNF $\alpha$  (Figure 1B) or LPS (Figure 1A). Finally, SUMO-1 modification was also seen with the endogenous NEMO (Figure 1C). These results together indicated that DNA-damaging agents induced signal-selective SUMO-1 conjugation of NEMO in a manner dependent on the ZF domain.

### Disruption of the Sumoylation Sites on NEMO

#### Abrogates DNA Damage-Dependent IKK Activation

Two lysine residues of NEMO, K277 and K309, conform to the proposed consensus motif  $\Psi$ KxD/E (where  $\Psi$  is a hydrophobic residue and x represents any residue) (Rodriguez et al., 2001) (Figure 2A). To determine if one of these lysines represented the *in vivo* SUMO-1 modification site, single (K277A and K309A) and double lysine to alanine (DK-mut) substitution mutants were constructed and examined as above. Although NEMO sumoylation was partially inhibited by single mutations (data not shown), DK-mut was not SUMO-1 modified (Figure 2B). While LPS was capable of inducing NEMO-associated IKK kinase activity in cells expressing either WT or DK-mut NEMO, VP16, or CPT could not activate IKK with DK-mut NEMO (Figure 2C). Accordingly, neither I $\kappa$ B $\alpha$  degradation nor NF- $\kappa$ B DNA binding activity was induced in the DK-mut cells upon stimulation with DNA damaging agents (Figure 2E). Single lysine mutants showed only mild inhibitory effects (Figure 2D), suggesting that the other intact lysine compensates for the

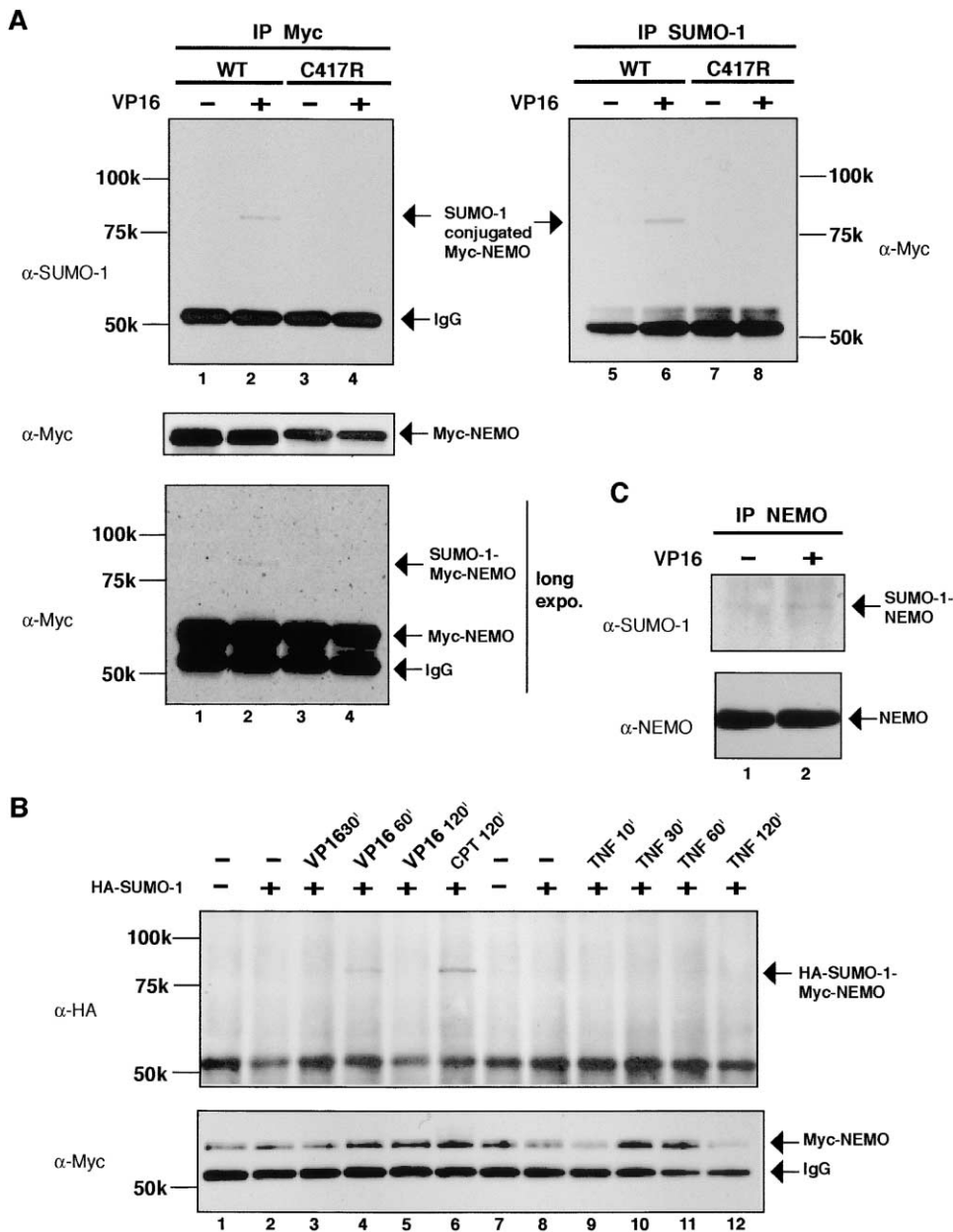


Figure 1. ZF-Dependent SUMO-1 Modification of NEMO

(A) NEMO-deficient 1.3E2 cells stably reconstituted with either Myc-tagged NEMO WT or a ZF point mutant (C417R) were left untreated or treated with VP16 (10  $\mu$ M) for 1 hr. Protein extracts were immunoprecipitated with either SUMO-1 or Myc antibodies and analyzed by Western blotting with either Myc or SUMO-1 antibodies.

(B) HEK293 cells stably expressing Myc-tagged NEMO were either transfected with vector control (lanes 1 and 7) or HA-SUMO-1 plasmid. 48 hr after transfection, the cells were left untreated or treated with VP16 as in (A), or CPT (10  $\mu$ M) or TNF $\alpha$  (10 ng/ml) for the indicated times. Protein extracts were immunoprecipitated with Myc antibody and immunoblotted with either HA or Myc antibodies.

(C) HEK293 cells untreated or treated with VP16 as above for 1 hr were then processed as above and immunoprecipitated with the NEMO antibody and immunoblotted with either SUMO-1 or NEMO antibody.

mutated lysine residue. Similar observations were made when two lysines were substituted with arginines (data not shown).

#### SUMO-1-Modified NEMO Accumulates in the Nucleus in Response to Genotoxic Stress

SUMO-1 modification may be associated with altered protein stability, but DNA damaging agents did not change the levels of NEMO (Figure 1C and others). Thus,

modulation of subcellular localization of WT and DK-mut proteins was next examined. Both WT and DK-mut proteins were predominantly localized in the cytoplasm of unstimulated cells (Figures 3A and 3B, upper and lower images). Surprisingly, many cells treated with VP16 showed evidence for nuclear staining of the WT NEMO proteins (Figures 3A and 3B). DK-mut NEMO remained cytoplasmic (Figures 3A and 3B), correlating with its lack of sumoylation (Figures 2B). LPS stimulation

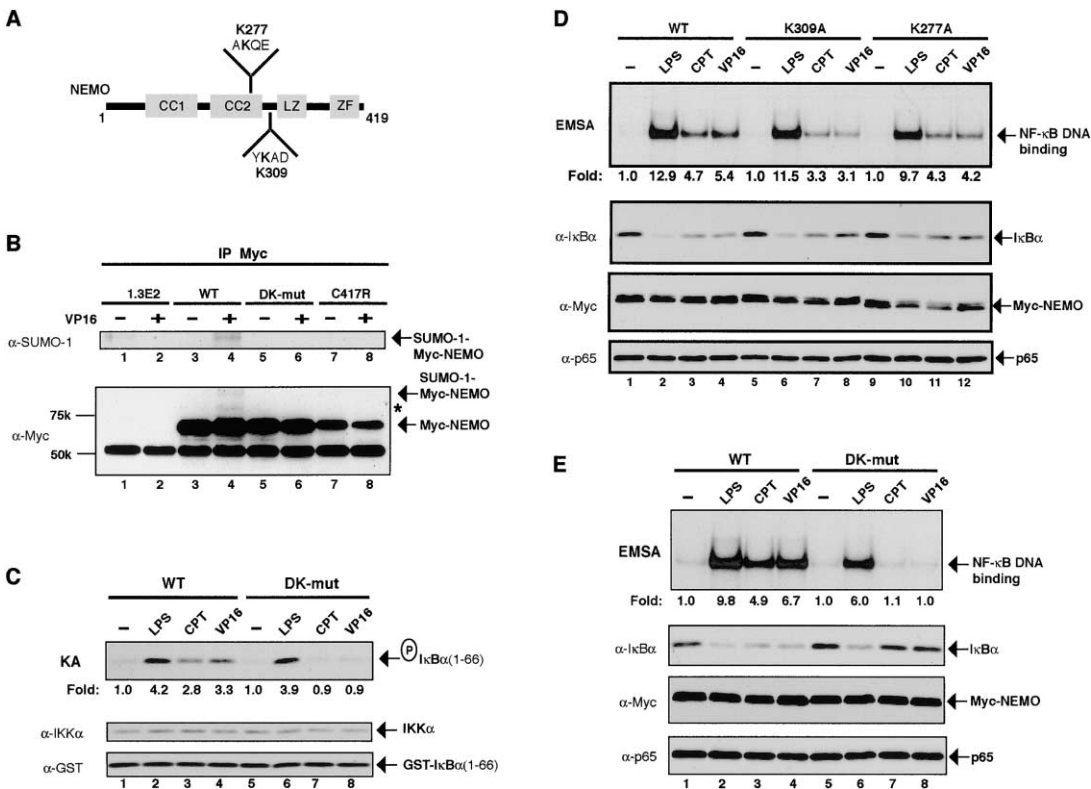


**Figure 2. Lysines 277 and 309 of NEMO Are Critical for SUMO-1 Modification and DNA Damage-Induced IKK and NF-κB Activation**  
**(A)** Schematic representation of NEMO and SUMO-1 modification sites (K277 and K309). Two coiled coil regions (CC1, CC2), leucine zipper (LZ), and ZF domains are shown.  
**(B)** The parental or 1.3E2 cells complemented with Myc-tagged WT, DK-mut, and C417R NEMO were either left untreated or treated with VP16 (10 μM, 60 min), and used for cell extracts preparation, immunoprecipitation with Myc antibody, and analysis by Western blotting with either SUMO-1 or Myc antibody.  
**(C)** 1.3E2 cells stably reconstituted with either Myc-tagged WT or DK-mut NEMO were left untreated or treated with LPS (20 μg/ml, 30 min), CPT (10 μM, 60 min), or VP16 (10 μM, 60 min). Protein extracts were immunoprecipitated with Myc antibody and subjected to a kinase assay. Immunoblotting with IKKα or GST antibody was performed with the kinase reactions as a loading control. Fold IKKα phosphorylation induction was measured using ImageQuant following exposure to Phosphorimager.  
**(D)** 1.3E2 cells stably reconstituted with either Myc-tagged NEMO WT or single lysine mutants (K277A and K309A) were untreated or treated with LPS (20 μg/ml, 60 min), CPT (10 μM, 120 min), or VP16 (10 μM, 120 min). Protein extracts were examined with EMSA and Western blotting using IKKα, Myc, and p65 antibodies. Fold induction of NF-κB DNA binding activity was measured as above.  
**(E)** DK-mut cells were treated and analyzed as in (A).

also did not alter the localization of these proteins (Figures 3A and 3B). Biochemical fractionation also supported nuclear accumulation of NEMO (Figure 3C). However, since SUMO-1 modification was labile without boiling cell samples, we were unable to detect sumoylated NEMO in these fractionation experiments that precluded prior boiling of cell samples in SDS. There was no detectable nuclear localization of the IKKα, unlike when cells were stimulated with certain cytokines (Anest et al., 2003; Yamamoto et al., 2003; also see below).

Expression constructs that tethered SUMO-1 to the N terminus of NEMO (Figure 4A) revealed that the WT, C417R, and DK-mut NEMO proteins displayed largely cytoplasmic localization (Figure 4B, 1-3, upper images), but SUMO-1 attachment resulted in their nuclear targeting (Figure 4B, compare images 1-3, upper and lower images). Thus, covalent modification by SUMO-1 could explain the nuclear localization of NEMO observed following DNA damage induction. Interestingly, when excess IKKβ catalytic subunit was coexpressed, SUMO-

NEMO became cytoplasmic (Figure 4B, images 4 and 5). Similarly, excess SUMO-NEMO did not change the cytoplasmic localization of IKKβ (Figure 4B, image 6). These observations implicated that only the IKK-unbound form of NEMO could accumulate in the nucleus upon SUMO-1 modification. To directly determine whether IKK association is dispensable for sumoylation, we disrupted this association with a cell-permeable NBD peptide (Figure 4C, compare lanes 12 and 13) and found that there was no impact on NEMO SUMO-1 modification (compare lanes 10 and 11). However, inhibition of NF-κB activation by DNA-damaging agents (Figure 4C, compare lanes 6-8) indicated that activation of NF-κB ultimately required the association of NEMO with IKK catalytic subunits (also see below).

SUMO-1 attachment to NEMO did not induce constitutive NF-κB activation when stably expressed in 1.3E2 (Figure 4D, lanes 1 and 5). LPS- and DNA damage-induced NF-κB activation was efficient in these cells (Figure 4D), indicating that SUMO did not impair the

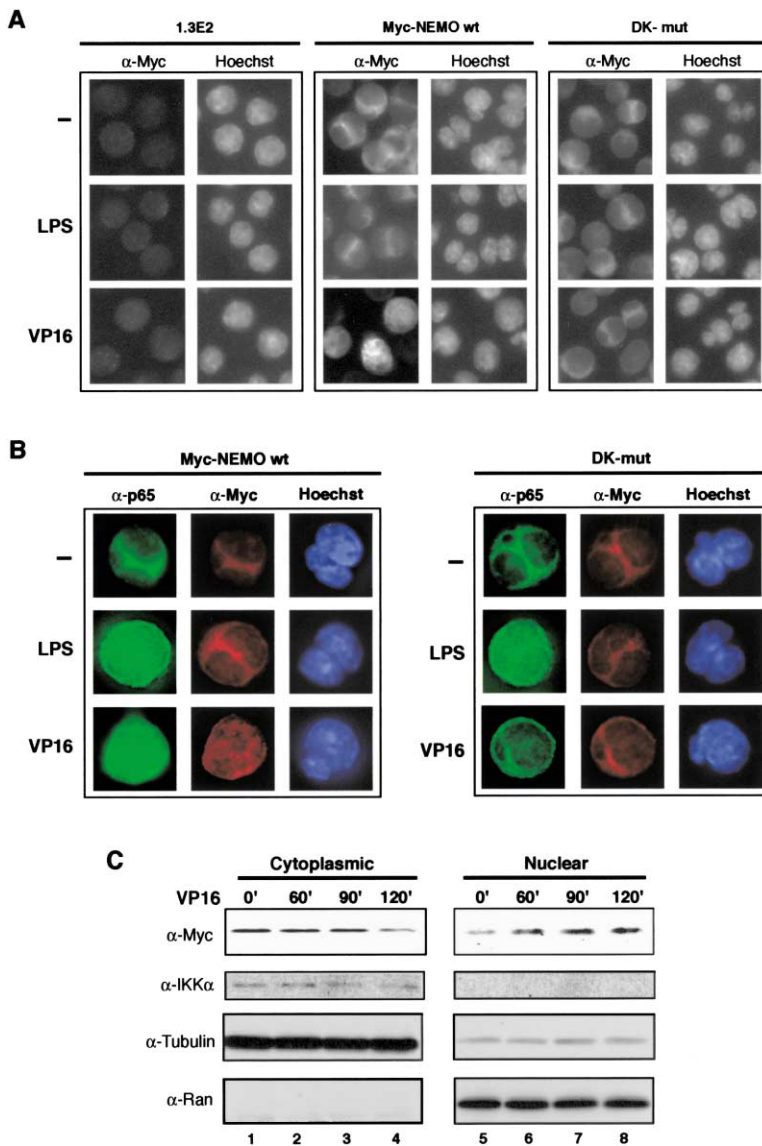


Figure 3. NEMO Localization to the Nucleus by Genotoxic Stress Depends on Intact Lys277 and 309

(A) Immunofluorescence of the 1.3E2 parental and those stably reconstituted with either Myc-tagged WT or DK-mut NEMO. Cells were untreated or treated with LPS (20  $\mu$ g/ml, 30 min) or VP16 (10  $\mu$ M, 90 min) and immunostained with the Myc antibody. Nuclei were visualized by Hoechst staining.

(B) Cells were treated as in (A) except the cells were costained with both p65 (green) or Myc (red) antibody and Hoechst dye (blue).

(C) HEK293 cells stably expressing Myc-NEMO were untreated or treated with VP16 at the indicated times. Cytoplasmic and nuclear extracts were generated and equivalent amounts of proteins were loaded on SDS-PAGE. Western blot analysis was done using the indicated antibodies.  $\alpha$ -Tubulin and Ran GTPase were shown for cytoplasmic and nuclear controls, respectively.

function of NEMO. Importantly, NF- $\kappa$ B signaling defects associated with ZF deficiency was compensated for by the SUMO-1 attachment (Figure 4E, compare lanes 4 and 9). Thus, SUMO-1 modification is both necessary and sufficient to overcome the NF- $\kappa$ B activation defects associated with mutations in the ZF domain of NEMO. However, unlike the ZF mutant, DK-mut deficiencies were not complemented by SUMO-1 (Figure 4E, compare lanes 12 and 15). These results suggested that SUMO-1 modification of NEMO was necessary but insufficient for DNA damage-induced NF- $\kappa$ B activation.

#### Lysines 277/309 of NEMO Are Necessary for Subsequent Modification by Ubiquitin Following DNA Damage Induction

We have on occasion noted that there were additional faint NEMO bands that appeared below the SUMO-1 modified band upon DNA damage induction, depending on time points analyzed (e.g., Figure 2B, asterisk). The size increase was on the order of 8–16 kDa, equivalent

to molecular weights of one or two ubiquitin molecules. Time course experiments showed the presence of at least two major modification bands—slower migrating band transiently peaking around 45 to 60 min and the other faster migrating one that became apparent around 60–90 min and remained detectable up to 120 min (Figure 5A, upper image). The slower migrating band was detectable by SUMO-1 antibody (Figure 5A, middle image), whereas ubiquitin antibody detected the other (Figure 5A, lower image). Even though Myc antibody detected the faster migrating band appearing at 45 min and peaking around 90 min, ubiquitin antibody only efficiently detected them at 90 min and somewhat less at 120 min time points. This difference in detection by Myc and ubiquitin antibodies is likely due to the inefficient detection of ubiquitylated NEMO by ubiquitin antibody. When similar time course samples were analyzed by EMSA, NF- $\kappa$ B activation was detectable at 60 min time and steadily increased to a peak at 120 min (Figure 5A, bottom image). This “peak” detection does not imply

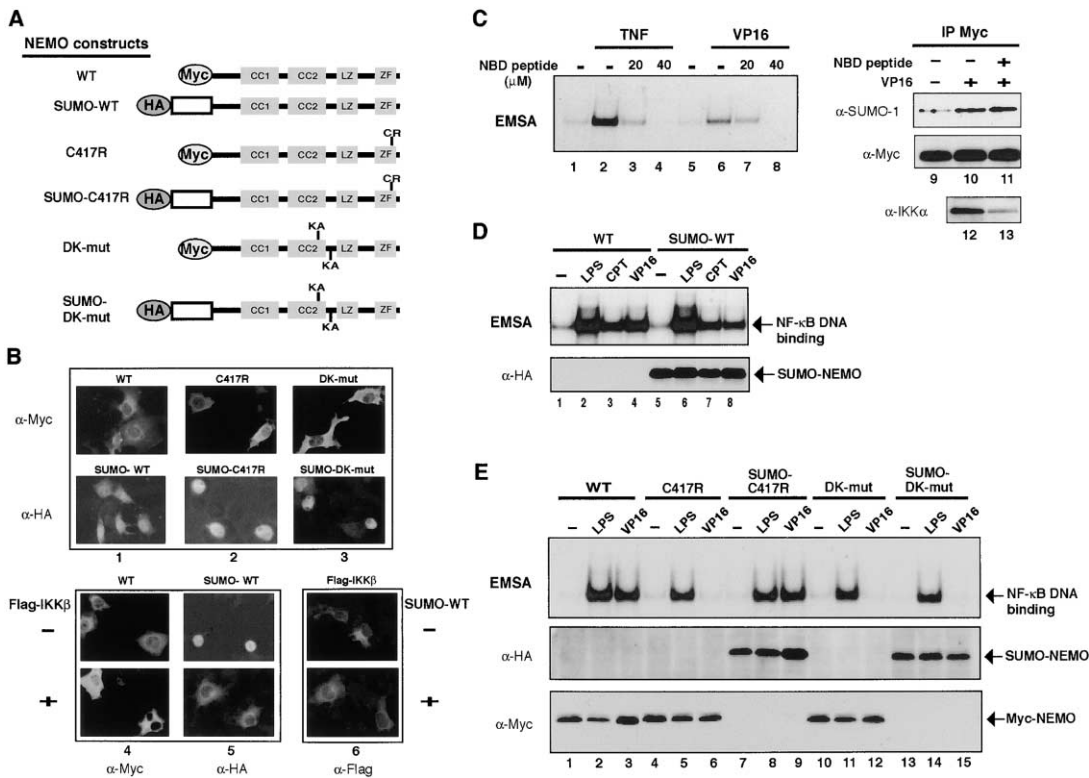


Figure 4. SUMO-1 Targets NEMO to the Nucleus

(A) Schematic diagrams of WT and mutant NEMO constructs N terminally fused to SUMO-1 lacking the C-terminal Gly-Gly residues. The SUMO-NEMO fusion constructs are HA tagged, and nonfusion NEMO constructs are Myc-tagged.

(B) Cos7 cells transfected with the indicated constructs were analyzed by immunofluorescence with Myc (pictures 1–3, upper images; and picture 4, upper and lower images), HA (pictures 1–3, lower images; and picture 5, upper and lower images), or Flag (picture 6) antibody. For lower images of pictures 4 and 5, four times the amount of the Flag-IKK $\beta$  construct was transfected in comparison to WT or SUMO-WT constructs. In picture 6, four times the amount of SUMO-WT construct was transfected in comparison to Flag-IKK $\beta$ .

(C) 1.3E2 cells stably reconstituted with Myc-tagged NEMO WT were pretreated with increasing concentration of cell-permeable NBD peptide and then stimulated with either TNF $\alpha$  (10  $\mu$ g/ml, 60 min) or VP16 (10  $\mu$ M, 60 min) as in Figure 1B. Samples were then analyzed by EMSA or immunoprecipitation as indicated. 20  $\mu$ M of NBD peptide was used for the IP samples. A low-level basal sumoylation of NEMO could be seen (lane 9), but the reason for this is unknown.

(D) 1.3E2 cells stably expressing Myc-NEMO-WT or SUMO-NEMO-WT were treated with LPS (20  $\mu$ g/ml, 30 min) or CPT (10  $\mu$ M, 120 min) and VP16 (10  $\mu$ M, 120 min). Protein extracts were analyzed with EMSA and Western blot.

(E) 1.3E2 cells stably expressing WT, C417R, and DK-mut NEMO or corresponding SUMO-fusion constructs were left untreated or treated with LPS (30 min) or VP16 (120 min) and the protein extracts were analyzed by EMSA and immunoblotting with either HA or Myc antibody.

the absence of modification leading to activation earlier than the peak time, as evidenced from the mild activation of NF- $\kappa$ B within 60 min. Nevertheless, these peak time points are consistent with the sequential events of sumoylation, ubiquitylation, and finally NF- $\kappa$ B activation.

Since direct conjugation of SUMO-1 to NEMO compensated for the ZF deficiency but failed to do so for the DK mutant (Figure 4E), we next evaluated whether these lysine residues were also required for ubiquitylation. Induction of slower migrating bands could be equally detected on both the SUMO-1-fused WT and ZF mutant of NEMO (Figure 5B, lanes 2–3 and 5–6). These slower bands could be detected by the ubiquitin antibody (data not shown), indicating that an intact ZF was not required for this modification. In contrast, ubiquitin conjugation was not seen with the SUMO-1 conjugated DK mutant (lanes 8–9). Thus, while SUMO-1 permitted nuclear accumulation of NEMO, lysine 277/309 were further required for subsequent ubiquitylation upon DNA

damage induction. Furthermore, consistent with the notion that transient sumoylation is the major rate-limiting step for NF- $\kappa$ B activation, constitutive presence of SUMO-NEMO protein permitted faster and longer activation kinetics compared to WT NEMO (Figure 5C; see Discussion).

#### ATM Is Dispensable for Sumoylation but Essential for Ubiquitylation of NEMO

Since DNA damaging conditions, especially those that induce DSBs, activate ATM and its related kinase ATR (Abraham, 2001), we next examined whether sumoylation and ubiquitylation of NEMO were regulated by these DNA damage-signaling kinases. We first evaluated the requirements of these kinases in NF- $\kappa$ B activation by VP16 treatment by employing the small interfering RNA strategy (siRNA) to knockdown their expression levels. Both siRNAs against ATM and ATR effectively and specifically reduced the expression of corresponding ki-

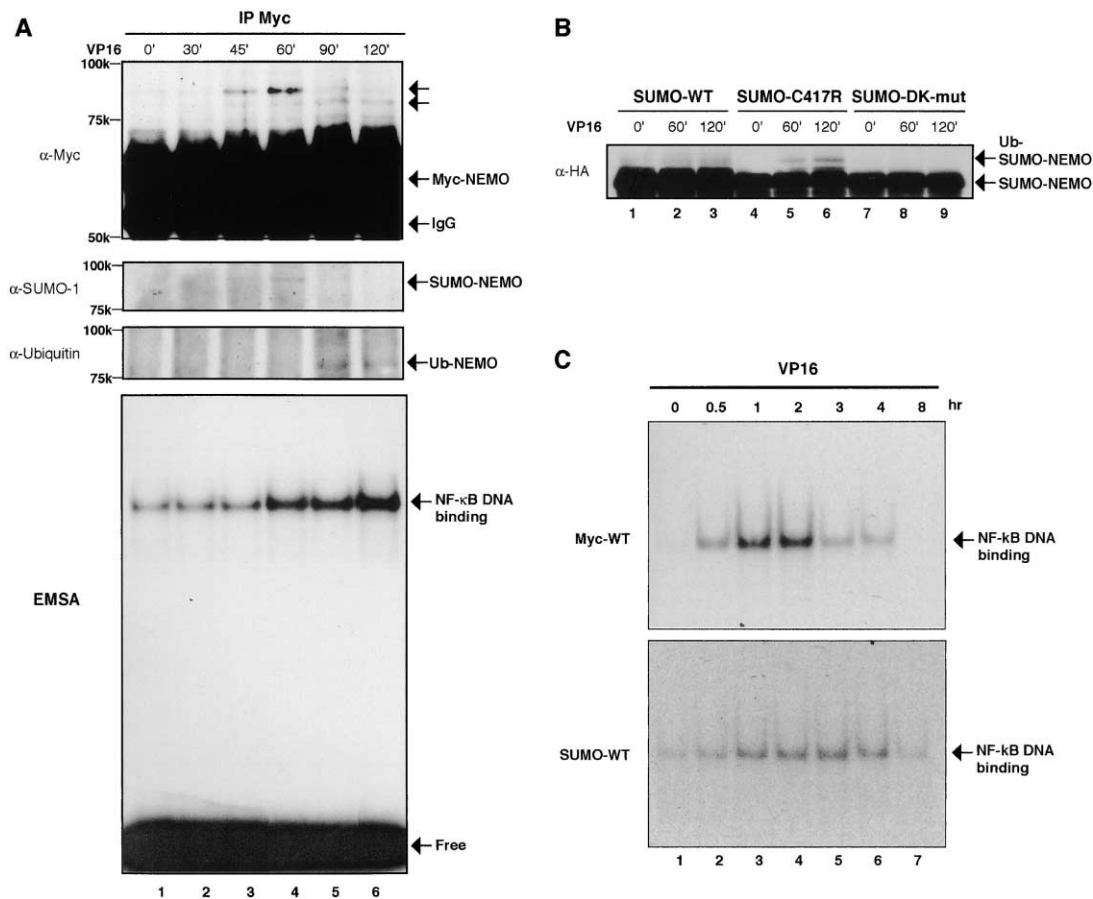


Figure 5. Sumoylation of NEMO Precedes Ubiquitylation and NF- $\kappa$ B Activation Following Genotoxic Stress

(A) 1.3E2 cells stably expressing Myc-NEMO-WT were treated with or without VP16 (10  $\mu$ M) for the indicated amount of time and used for immunoprecipitation experiments to detect ubiquitylated and sumoylated NEMO, using the indicated antibodies for Western blot analysis. Arrows in the upper image point to corresponding bands detected in the middle and lower images. The similar time course samples were prepared for EMSA analysis to detect NF- $\kappa$ B activation.

(B) 1.3E2 cells expressing SUMO-WT, SUMO-C417R, or SUMO-DK-mut were treated with VP16 (10  $\mu$ M) for the following time intervals and processed for immunoprecipitation followed by Western blot analysis using HA antibody.

(C) Myc-NEMO-WT and SUMO-NEMO-WT cells were treated with VP16 (10  $\mu$ M) for indicated times and analyzed by EMSA as above.

nases, but only ATM-deficiency completely and selectively blocked NF- $\kappa$ B activation by VP16 (Figure 6A, left images). ATR deficiency had no inhibitory impacts on either of these activation pathways (right images). Surprisingly, in contrast to complete inhibition of NF- $\kappa$ B activation, NEMO sumoylation was hardly affected by ATM deficiency when compared to CHK1-deficiency control (Figure 6B, compare lanes 5 and 6). Importantly, ATM-deficiency caused complete loss of NEMO ubiquitylation (Figure 6C, compare lanes 2 and 4). Thus, these studies revealed a surprising finding that ATM regulated ubiquitylation, but not sumoylation, of NEMO to permit the NF- $\kappa$ B pathway. Moreover, NEMO became phosphorylated upon genotoxic stress induction, which was prevented by the ATM inhibitor wortmannin (Figures 6D and 6E). These results suggested that ATM regulated NEMO phosphorylation and ubiquitylation.

#### Activation of IKK by DNA Damage Is Ultimately a Cytoplasmic Event

Even though we did not observe evidence for nuclear IKK $\alpha$  upon genotoxic stress (Figure 3C), the potential

for this catalytic subunit to appear in the nucleus (Anest et al., 2003; Yamamoto et al., 2003) raised the possibility that a small fraction of nuclear IKK complex might have mediated NF- $\kappa$ B activation in the nucleus. This was a critical issue, since NF- $\kappa$ B/I $\kappa$ B $\alpha$  complexes constitutively shuttle between the cytoplasm and the nucleus to afford potential intranuclear activation reactions. We first selectively caused nuclear localization of I $\kappa$ B $\alpha$ /NF- $\kappa$ B, but not I $\kappa$ B $\beta$ /NF- $\kappa$ B, complexes by a brief exposure to the CRM1 inhibitor leptomycin B (LMB) (Huang and Miyamoto, 2001) and then examined whether or not the former were selectively targeted for activation by IKK following DNA damage induction. As expected, the inhibition of nuclear export by LMB did not affect TNF $\alpha$ -induced activation of IKK (Figure 7A, lane 3). In keeping with the concept that TNF $\alpha$  activation of IKK is a cytoplasmic event, TNF $\alpha$  caused degradation of cytoplasmic I $\kappa$ B $\beta$ , but not nuclear I $\kappa$ B $\alpha$  following LMB exposure (Figure 7B, lane 3, middle and lower images). This resulted in the partial loss of NF- $\kappa$ B activation (Figure 7B, lane 3, upper image). Importantly, LMB also did not interfere with the activation of NEMO-associated IKK by VP16 or

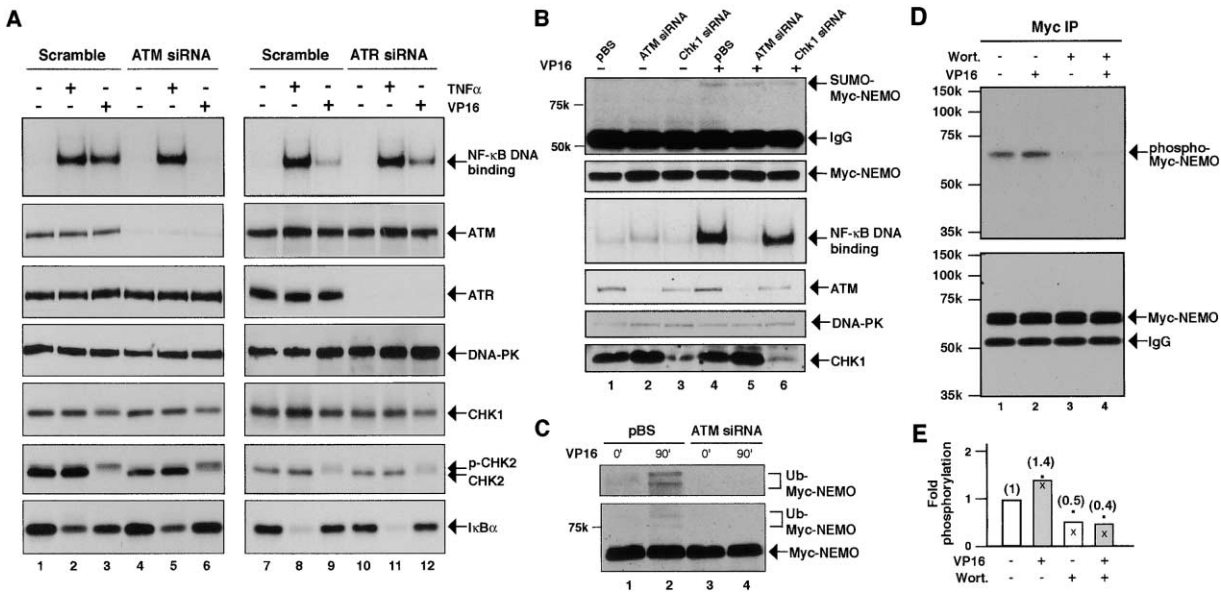


**Figure 6. ATM Regulates NEMO Ubiquitylation, but Not Sumoylation, Following Genotoxic Stress Induction**  
 (A) HEK293 cells were transfected with either scrambled siRNA (lanes 1–3 and 7–9) or siRNA targeted against ATM (lanes 4–6) or ATR (lanes 10–12). Twenty-four hours after transfection, cells were treated with TNF $\alpha$  (10 ng/ml) or VP16 (10  $\mu$ M, lanes 3 and 6; 1  $\mu$ M, lanes 9 and 12) for 120 min and total cell extracts were prepared and analyzed by EMSA and parallel Western blotting using corresponding antibodies as shown. Similar effects were seen with siRNA against ATR at 10  $\mu$ M VP16 (data not shown).  
 (B) HEK293 cells stably expressing Myc-NEMO-WT were cotransfected with a HA-SUMO construct and siRNA against ATM or CHK1, treated with VP16 (60 min for the upper two images and 120 min for the last four images), and processed for EMSA and Western blot analysis.  
 (C) HEK293 cells stably expressing Myc-NEMO-WT were transfected with a HA-ubiquitin construct, treated with VP16 for 90 min and processed for immunoprecipitation and Western blot analysis using HA (upper image) and Myc (lower image) antibodies.  
 (D) 1.3E2 cells stably expressing Myc-NEMO-WT were labeled with ortho- $^{32}$ P and stimulated with VP16 (20  $\mu$ M, 60 min) in the presence and absence of wortmannin (20  $\mu$ M), and processed for immunoprecipitation using Myc antibody. Myc-NEMO was transferred to membrane, exposed to a Phosphorimager screen, and analyzed by ImageQuant (upper image). The membrane was then analyzed by Western blotting using Myc antibody (lower image).  
 (E) The intensities of phosphorylated NEMO in D were quantified by ImageQuant from two independent experiments (denoted as  $\bullet$  and  $\times$ ) and displayed as fold-phosphorylation. The data from experiment “x” is shown in (D). The numbers in the parentheses represent the average values. The reduction of basal phosphorylation of NEMO by wortmannin indicates that stress from ortho- $^{32}$ P labeling likely caused ATM activation to increase basal phosphorylation of NEMO.

CPT treatment (Figure 7A, lane 6, others not shown), indicating that the CRM1 export system is not required for IKK activation by nuclear DNA damage. Moreover, only cytoplasmic I $\kappa$ B $\beta$  is inducibly degraded upon exposure to VP16 and CPT (Figure 7B, lanes 6 and 9, middle and lower images). This selective degradation of I $\kappa$ B $\beta$  again resulted in partial activation of NF- $\kappa$ B (Figure 7B, lanes 3, 6, and 9, upper image). Collectively, our results indicated that even though free NEMO was first translocated to the nucleus in association with SUMO-1 modification and then modified by ubiquitylation in an ATM-dependent fashion, the IKK kinase activity that was subsequently associated with NEMO was present in the cytoplasm to activate NF- $\kappa$ B.

**Discussion**

Despite the vast knowledge accumulating from studies focusing on signal transduction pathways emanating from cell surface receptors, very little is understood regarding nuclear-to-cytoplasmic signaling pathways. A nuclear “priming” of Ste5, a scaffold for the yeast MAPK pathway, has been found to be required for activation of this system from cell surface receptors (Mahanty et

al., 1999). Additionally, TR3, an orphan nuclear receptor, was shown to rapidly translocate from the nucleus to the cytoplasm and finally to mitochondria following exposure to apoptosis inducing agents (Li et al., 2000). Even though these studies highlighted the existence of molecular communication pathways from the nucleus to the cytoplasm, the signaling mechanisms or the nature of the “priming” events remain to be elucidated.

In the NF- $\kappa$ B signaling pathways, NEMO plays an essential role by permitting physiological regulation of the cytoplasmic IKK complex. However, biochemical events that are necessary for NEMO to regulate IKK activity are still unclear. In this study, we delineated sequential regulatory posttranslational modifications of NEMO upon genotoxic stress induction, which begins with SUMO-1 conjugation. This modification was transient, signal selective, and not evident with LPS or TNF $\alpha$  stimulation. The signal specificity was in part due to the requirement of the C-terminal ZF domain of NEMO for SUMO-1 modification. The ZF is required for NF- $\kappa$ B activation by DNA damaging agents, but is dispensable for activation by LPS (Huang et al., 2002). We further found that direct attachment of SUMO-1 to NEMO was sufficient to localize NEMO to the nucleus and overcome the ZF defi-



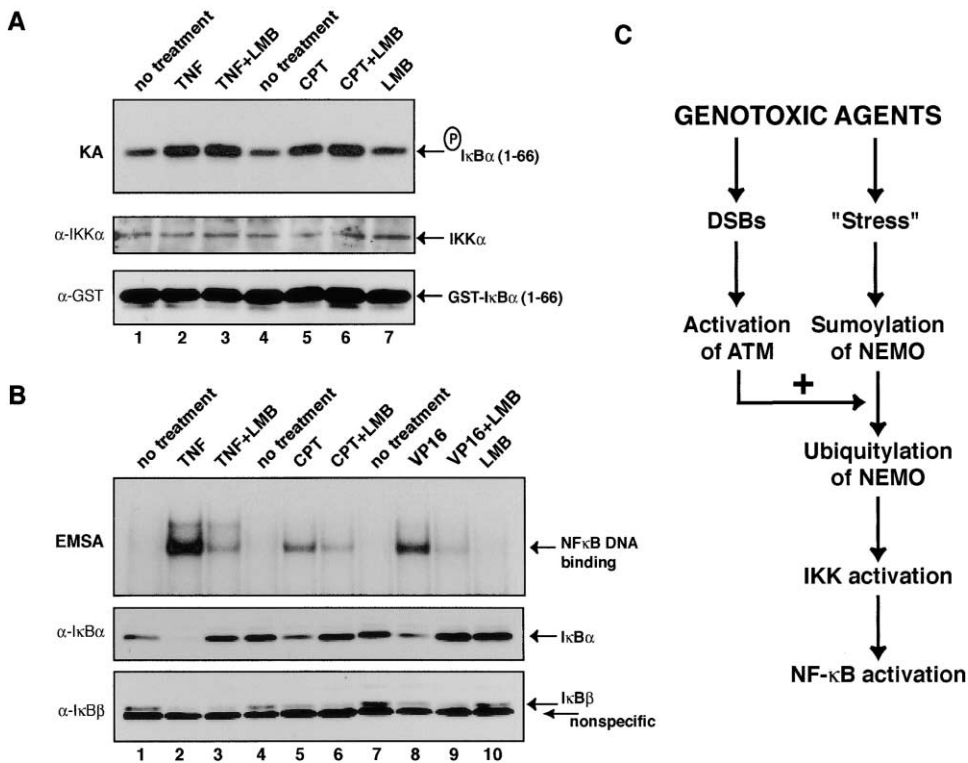


Figure 7. NEMO-Associated and DNA-Damage-Activated IKK is Cytoplasmic

(A) CEM cells were exposed for 60 min to LMB (20 ng/ml, lanes 3, 6, and 7) and unstimulated or stimulated with either TNF $\alpha$  (10 ng/ml) for 15 min (lanes 2 and 3) or CPT (10  $\mu$ M) for 60 min (lanes 5 and 6). Protein extracts were then immunoprecipitated with NEMO antibody and analyzed for phosphorylation of GST-I $\kappa$ B $\alpha$  (1-66) using  $\gamma$ - $^{32}$ P-ATP. The kinase reactions were electrophoresed, transferred to membranes, exposed to Phosphorimager screens, and then analyzed by IKK $\alpha$  or GST antibody for loading control.

(B) CEM cells were untreated or pretreated with LMB for 60 min (lanes 3, 6, and 9) and then stimulated with TNF $\alpha$  for 30 min (lanes 2 and 3), or CPT (lanes 5 and 6) or VP16 (10  $\mu$ M; lanes 8 and 9) for 120 min, and processed for EMSA and Western blot analyses using I $\kappa$ B $\alpha$  and I $\kappa$ B $\beta$  antibodies.

(C) Schematic diagram depicting a model for coordinate regulation of NEMO ubiquitylation by sumoylation and ATM activation following genotoxic stress induction.

ciency. These studies indicated that the only critical function of the ZF domain in the context of DNA damage signaling was to permit sumoylation of NEMO and further that the precise location of SUMO-1 did not have to be at lysine 277 or 309. Similar approaches have been used to study the role of ubiquitin in VP16 transactivation (Salghetti et al., 2001) and SUMO-1 in Sp3-dependent transcription (Ross et al., 2002). It is interesting to note that SUMO deconjugation was previously implicated in inhibition of cytokine-induced NF- $\kappa$ B activation by the Yersinia YopJ protein (Orth et al., 2000), but the nature of SUMO substrate(s) remains to be determined.

Our data are consistent with the model in which NEMO is in a dynamic flux between free and IKK-associated states and that genotoxic stress causes the nuclear appearance of free NEMO. The dynamic NEMO association with the IKK subunits is consistent with the rapid disruption of the complex by the addition of the NBD peptide derived from IKK $\beta$  (May et al., 2000). This NBD peptide also did not block the SUMO-1 modification of NEMO by genotoxic stress, further supporting the notion that free NEMO is sumoylated. SUMO-1 modification of NEMO is necessary but insufficient to induce IKK and NF- $\kappa$ B activation since SUMO-1 conjugation was insuffi-

cient to bypass the NF- $\kappa$ B activation deficiency of the NEMO DK mutant. Similar to site-specific competition between sumoylation and ubiquitylation on certain substrates (Desterro et al., 1998; Hoege et al., 2002), ubiquitylation of NEMO was also dependent on intact lysine 277/309. Moreover, the mobility of ubiquitylated NEMO on SDS-PAGE was faster than that of the sumoylated one, suggesting ubiquitylated NEMO was devoid of SUMO-1. Thus, sumoylation is necessary to cause nuclear accumulation of NEMO, but it appears to be desumoylated prior to or in conjunction with subsequent ubiquitylation reaction.

The role of mutually exclusive modifications of a specific lysine residue of PCNA by SUMO-1 and ubiquitin has recently been found to play a critical role in DNA damage repair and DNA replication (Hoege et al., 2002). There are number of DNA damage signaling and repair proteins that have ubiquitin conjugating or ligase motifs, including RAD6, RAD18, UBC13, UEV1A, BRCA1/BARD1 complex, among others (Abraham, 2001; Kastan and Lim, 2000; Zhou and Elledge, 2000). It is yet to be determined how genotoxic stress regulates their enzymatic activity and substrate selectivity. Moreover, it is also unclear how modification of the same lysine residue(s)

by SUMO-1 and ubiquitin is enzymatically regulated. Our study provided a surprising observation that ATM regulates only ubiquitylation, but not sumoylation, in the case of NF- $\kappa$ B activation pathway. While ATM was implicated in NF- $\kappa$ B activation by certain genotoxic stimuli, such as ionizing radiation (Li et al., 2001), the manner in which ATM regulates this pathway remained mysterious. Our observations together indicated that genotoxic stress induces two separate signaling pathways to regulate NEMO ubiquitylation (Figure 7C). Coordinate activation of both of these pathways by genotoxic stress—NEMO sumoylation and ATM activation—is necessary to permit NEMO ubiquitylation to ultimately activate IKK and NF- $\kappa$ B. This notion is consistent with the observation that attachment of SUMO-1 to NEMO or overexpression of ATM is insufficient for NF- $\kappa$ B activation (Figure 4D and S.M.W.-D, unpublished data). Recent studies by Vierstra and colleagues have found that a variety of stresses, such as oxidative stress and heat shock, cause transient sumoylation of a multitude of substrates in *Arabidopsis* (Kurepa et al., 2003). Stress-dependent sumoylation of different substrates has also been observed in mammalian cells (Hietakangas et al., 2003; Mao et al., 2000; Rodriguez et al., 1999; Rui et al., 2002). Thus, it is probable that transient SUMO modification of NEMO by genotoxic stress is due to a stress-signaling pathway unrelated to DNA damage per se. In contrast, NEMO ubiquitylation seems to require a separate signaling pathway from DNA double-strand break to ATM activation. Moreover, NEMO is phosphorylated upon DNA damage induction in vivo that is completely inhibited by an ATM inhibitor. ATM siRNA did not increase the detection of steady-state levels of sumoylated NEMO following genotoxic stress. This suggested that ATM was not required for desumoylation; otherwise, the accumulation of sumoylated NEMO would be expected without ATM. Kinetics of NF- $\kappa$ B activation by genotoxic stress was transient, like sumoylation. However, ATM activation is documented to be very prompt and persistent following DNA damage induction (Bakkenist and Kastan, 2003). When SUMO-NEMO fusion was supplied constitutively to overcome the necessity of sumoylation, NF- $\kappa$ B activation reached the maximal level faster and persisted much longer. Thus, one can modulate the time course of NF- $\kappa$ B activation by genotoxic stress conditions by bypassing the major rate-limiting SUMO step. Identification of NEMO phosphorylation site(s), and specific ubiquitin E2 and E3, along with specific SUMO E3 and hydrolase, will be required to determine how sumoylation and ATM activation coordinate NEMO ubiquitylation following genotoxic stress. These studies may also help link the above NEMO modifications with the RIP kinase that was recently implicated in a genotoxic stress-dependent activation of NF- $\kappa$ B (Hur et al., 2003). These studies may also help sort out different conflicting events implicated in NF- $\kappa$ B activation by genotoxic agents (Criswell et al., 2003) into those induced by DNA damage per se and those related to other stresses induced by these agents without involving damage to the DNA.

While SUMO-1 modification is involved in nuclear localization of NEMO and subsequent ubiquitylation, the ultimate IKK and NF- $\kappa$ B activation was found to be cytoplasmic. The simplest interpretation is to consider free

NEMO as the, or a component of, DNA damage-induced nuclear-to-cytoplasmic signal for the NF- $\kappa$ B activation pathway. However, based on immunostaining and biochemical fractionation analyses, we were unable to observe a large-scale exit of NEMO out of the nucleus prior to NF- $\kappa$ B activation. This is likely due to a technical issue based on the consideration that a fraction of nuclear NEMO may become ubiquitylated and exported out of the nucleus. Consistent with this notion, prevention of NEMO nuclear exit by the attachment of the nuclear localization signal of SV40 large T antigen prevented NF- $\kappa$ B activation when reconstituted in 1.3E2 cells (T.H., unpublished data). There is now emerging evidence that IKK activation may involve upstream ubiquitylation of signaling components, such as TRAF2, TRAF6, and NEMO, but the precise mechanisms involved have not been revealed (Brummelkamp et al., 2003; Deng et al., 2000; Kovalenko et al., 2003; Trompouki et al., 2003; Wang et al., 2001). It is of great interest to determine how ubiquitylation of NEMO plays a role in IKK activation upon DNA damage induction.

Since NF- $\kappa$ B has emerged as a key determinant for cellular sensitivity to anticancer drugs and radiation treatments (Karin et al., 2002), the sequential posttranslational modifications of NEMO by SUMO-1 and ubiquitin may also provide pathway-selective targets to enhance anticancer therapy. Our important future goals include the identification of molecular components and their regulatory mechanisms involved in these modifications of NEMO in the NF- $\kappa$ B genotoxic signal transduction pathway to identify relevant targets for cancer treatment.

## Experimental Procedures

### Plasmids

Myc-NEMO was described previously (Huang et al., 2002). Generation of point mutations of NEMO at lysines 277 and/or 309 to alanines or arginines were done by two-step PCR mutagenesis from the original NEMO template and verified by DNA sequencing. To generate HA-tagged SUMO-1-NEMO fusion constructs, SUMO-1 (amino acids 1–96) was amplified by PCR and cloned into the 2 $\times$  HA pcDNA3 vector (Invitrogen). NEMO was then amplified by PCR and cloned downstream of SUMO-1 in frame.

### Reagents and Antibodies

VP16, CPT and bacterial LPS were purchased from Sigma and human recombinant TNF $\alpha$  was from Calbiochem. IgGs against IKK $\alpha$  (M280), c-Myc (9E10), NEMO (M-18), I $\kappa$ B $\alpha$  (C-21), p65 (C-20), DNAPK (C-19), CHK1 (Fl-476), CHK2 (H-300), and GST (B-14) were purchased from Santa Cruz Biotechnology. Anti-SUMO-1 (anti-GMP1) was from Zymed Laboratories, anti-Flag (M2) was from Sigma, anti-HA.11 and antiubiquitin were from Covance, and anti-ATM (2C1) was from GeneTex. Anti-ATR polyclonal rabbit IgG was a gift from Dr. R. Tibbetts (Tibbetts et al., 2000). Antirabbit and antimouse antibodies and Protein-A, each conjugated to horseradish peroxidase, were obtained from Amersham Pharmacia Biotech. The cell permeable NBD peptide (May et al., 2000) was purchased from BIOMOL. Cell and extract preparations for EMSA and Western blot analyses were described previously (Huang et al., 2000a). Cytoplasmic and nuclear extracts from HEK293 cells were prepared as described previously (Miyamoto et al., 1998). siRNA-mediated interference to downregulate ATM, ATR, or Chk1 expression in HEK293 cells (35 mm dishes) was done by transfecting 200 pmoles each of SMARTpool double-stranded RNA oligonucleotides (Dharmacon) or scramble siRNA (+ strand, 5'-AAUACCGUCUCCACUUGAUCGdT-3'; - strand, 5'-CGAUAAGUGGAGACGGUAdTdT-3') using a calcium-phosphate method as previously described (Huang et al., 2000a).

#### Cell Culture and Generation of Stable Transfectants

1.3E2 murine pre-B and its derivatives, Cos7, HEK293, and CEM cells were grown as described previously (Huang et al., 2002). Transient transfection of plasmid DNA in HEK293 or Cos-7 cells was done using standard calcium phosphate precipitation method (Huang et al., 2000a). 1.3E2 cells were reconstituted with Myc- or HA-tagged NEMO WT or mutants by electroporation and selection with G418 (1 mg/ml) as described previously (Huang et al., 2002).

#### Kinase Assay and Immunoprecipitation

The IKK kinase assay was described previously (Huang et al., 2002). Samples for IP experiments were done as described above except for immediate boiling in 1% SDS for 15 min followed by dilution with the IP buffer to 0.1% SDS prior to immunoprecipitation.

#### Immunostaining

1.3E2 pre-B and Cos7 cell lines were cultured in four-well chamber slides (LAB-TEK II CC2 treated or LAB-TEK), stimulated, and then processed as described previously (Huang et al., 2002) using appropriate primary antibodies (1:250). DNA was visualized by Hoechst 33342 (Molecular Probes) staining. Cells were mounted with Prolong Antifade (Molecular Probes), visualized, and photographed using a Zeiss Axioplan epifluorescence microscope with the aid of fluorescein or rhodamine-specific filters.

#### In Vivo Ortho-<sup>32</sup>P Labeling of NEMO

$1 \times 10^7$  1.3E2 cells stably expressing Myc-NEMO-WT were incubated for 2 hr at 37°C under 10% CO<sub>2</sub> with 1.5 mCi of sodium ortho-<sup>32</sup>P (ICN Pharmaceutical, Inc.) in 1 ml of phosphate-free DMEM in the presence of 10% fetal calf serum previously dialyzed against excess Tris-buffered saline. Cells were then stimulated for 60 min, washed with ice-cold PBS, lysed in 1% SDS in the IP buffer above containing protease inhibitors and phosphatase inhibitors as described (Huang et al., 2002), boiled for 10 min, and then processed for immunoprecipitation as above. Myc-NEMO was released by boiling and reimmunoprecipitated to reduce background signals. Final immunoprecipitates were transferred to Immobilon-P membrane following 10% SDS-PAGE, exposed to a Phosphorimager screen, and analyzed by the ImageQuant program. The membranes were then processed for Western blot analysis with an anti-Myc-antibody to ensure equivalent IP efficiency.

#### Acknowledgments

We thank Z.J. Chen for Myc-tagged WT NEMO expression construct, I. Verma for flag-tagged IKK $\beta$ /2 construct; S. Shumway and Y. Xiong for HA pcDNA3 vector and SUMO-1 cDNA constructs; R. Tibbetts for ATR antibody; B. Seufzer for technical support; and Drs. K. Orth, Z. Chen, R. Tibbetts, R. Anderson, and R. Vierstra and the Miyamoto lab members for helpful discussions. This work was supported in part by the Herman I. Shapiro Fellowship through the University of Wisconsin Medical School to T.T.H.; the Department of Defense Predoctoral Fellowship BC010767 to S.M.D.; and NIH R01-CA077474 and R01-CA081065 to S.M.

Received: April 21, 2003

Revised: October 28, 2003

Accepted: October 28, 2003

Published: November 25, 2003

#### References

Abraham, R.T. (2001). Cell cycle checkpoint signaling through the ATM and ATR kinases. *Genes Dev.* 15, 2177–2196.  
Anest, V., Hanson, J.L., Cogswell, P.C., Steinbrecher, K.A., Strahl, B.D., and Baldwin, A.S. (2003). A nucleosomal function for I $\kappa$ B kinase- $\alpha$  in NF- $\kappa$ B-dependent gene expression. *Nature* 423, 659–663.  
Baeuerle, P.A., and Baltimore, D. (1988). I $\kappa$ B: a specific inhibitor of the NF- $\kappa$ B transcription factor. *Science* 242, 540–546.  
Bakkenist, C.J., and Kastan, M.B. (2003). DNA damage activates ATM through intermolecular autophosphorylation and dimer dissociation. *Nature* 421, 499–506.  
Brummelkamp, T.R., Nijman, S.M., Dirac, A.M., and Bernards, R.

(2003). Loss of the cylindromatosis tumour suppressor inhibits apoptosis by activating NF- $\kappa$ B. *Nature* 424, 797–801.

Criswell, T., Leskov, K., Miyamoto, S., Luo, G., and Boothman, D.A. (2003). Transcription factors activated in mammalian cells after clinically relevant doses of ionizing radiation. *Oncogene* 22, 5813–5827.

Deng, L., Wang, C., Spencer, E., Yang, L., Braun, A., You, J., Slaughter, C., Pickart, C., and Chen, Z.J. (2000). Activation of the I $\kappa$ B kinase complex by TRAF6 requires a dimeric ubiquitin-conjugating enzyme complex and a unique polyubiquitin chain. *Cell* 103, 351–361.

Desterro, J.M., Rodriguez, M.S., and Hay, R.T. (1998). SUMO-1 modification of I $\kappa$ B $\alpha$  inhibits NF- $\kappa$ B activation. *Mol. Cell* 2, 233–239.

Devary, Y., Gottlieb, R.A., Smeal, T., and Karin, M. (1992). The mammalian ultraviolet response is triggered by activation of Src tyrosine kinases. *Cell* 71, 1081–1091.

Doffinger, R., Smahi, A., Bessia, C., Geissmann, F., Feinberg, J., Durandy, A., Bodemer, C., Kenwrick, S., Dupuis-Girod, S., Blanche, S., et al. (2001). X-linked anhidrotic ectodermal dysplasia with immunodeficiency is caused by impaired NF- $\kappa$ B signaling. *Nat. Genet.* 27, 277–285.

Ghosh, S., and Karin, M. (2002). Missing pieces in the NF- $\kappa$ B puzzle. *Cell* 109 (Suppl), S81–S96.

Hietakangas, V., Ahlskog, J.K., Jakobsson, A.M., Hellesuo, M., Sahlberg, N.M., Holmberg, C.I., Mikhailov, A., Palvimo, J.J., Pirkkala, L., and Sistonen, L. (2003). Phosphorylation of serine 303 is a prerequisite for the stress-inducible SUMO modification of heat shock factor 1. *Mol. Cell. Biol.* 23, 2953–2968.

Hoege, C., Pfander, B., Moldovan, G.L., Pyrowolakis, G., and Jentsch, S. (2002). RAD6-dependent DNA repair is linked to modification of PCNA by ubiquitin and SUMO. *Nature* 419, 135–141.

Huang, T.T., and Miyamoto, S. (2001). Postrepression activation of NF- $\kappa$ B requires the amino-terminal nuclear export signal specific to I $\kappa$ B $\alpha$ . *Mol. Cell. Biol.* 21, 4737–4747.

Huang, T.T., Wuerzberger-Davis, S.M., Seufzer, B.J., Shumway, S.D., Kurama, T., Boothman, D.A., and Miyamoto, S. (2000a). NF- $\kappa$ B activation by camptothecin: a linkage between nuclear DNA damage and cytoplasmic signaling events. *J. Biol. Chem.* 275, 9501–9509.

Huang, T.T., Kudo, N., Yoshida, M., and Miyamoto, S. (2000b). A nuclear export signal in the N-terminal regulatory domain of I $\kappa$ B $\alpha$  controls cytoplasmic localization of the inactive NF- $\kappa$ B/I $\kappa$ B $\alpha$  complexes. *Proc. Natl. Acad. Sci. USA* 97, 1014–1019.

Huang, T.T., Feinberg, S.L., Suryanarayanan, S., and Miyamoto, S. (2002). The zinc finger domain of NEMO is selectively required for NF- $\kappa$ B activation by UV radiation and topoisomerase inhibitors. *Mol. Cell. Biol.* 22, 5813–5825.

Hunter, T. (2000). Signaling—2000 and beyond. *Cell* 100, 113–127.

Hur, G.M., Lewis, J., Yang, Q., Lin, Y., Nakano, H., Nedospasov, S., and Liu, Z.G. (2003). The death domain kinase RIP has an essential role in DNA damage-induced NF- $\kappa$ B activation. *Genes Dev.* 17, 873–882.

Jain, A., Ma, C.A., Liu, S., Brown, M., Cohen, J., and Strober, W. (2001). Specific missense mutations in NEMO result in hyper-IgM syndrome with hypohydrated ectodermal dysplasia. *Nat. Immunol.* 2, 223–228.

Karin, M., and Hunter, T. (1995). Transcriptional control by protein phosphorylation: signal transmission from the cell surface to the nucleus. *Curr. Biol.* 5, 747–757.

Karin, M., Cao, Y., Greten, F.R., and Li, Z.W. (2002). NF- $\kappa$ B in cancer: from innocent bystander to major culprit. *Nat. Rev. Cancer* 2, 301–310.

Kastan, M.B., and Lim, D.S. (2000). The many substrates and functions of ATM. *Nat. Rev. Mol. Cell Biol.* 1, 179–186.

Kovalenko, A., Chable-Bessia, C., Cantarella, G., Israel, A., Wallach, D., and Courtois, G. (2003). The tumour suppressor CYLD negatively regulates NF- $\kappa$ B signaling by deubiquitination. *Nature* 424, 801–805.

Kurepa, J., Walker, J.M., Smalle, J., Gosink, M.M., Davis, S.J., Durham, T.L., Sung, D.Y., and Vierstra, R.D. (2003). The small ubiquitin-like modifier (SUMO) protein modification system in Arabidopsis. Accumulation of SUMO1 and -2 conjugates is increased by stress. *J. Biol. Chem.* 278, 6862–6872.

- Li, N., and Karin, M. (1998). Ionizing radiation and short wavelength UV activate NF- $\kappa$ B through two distinct mechanisms. *Proc. Natl. Acad. Sci. USA* **95**, 13012–13017.
- Li, Q., and Verma, I.M. (2002). NF- $\kappa$ B regulation in the immune system. *Nat. Rev. Immunol.* **2**, 725–734.
- Li, H., Kolluri, S.K., Gu, J., Dawson, M.I., Cao, X., Hobbs, P.D., Lin, B., Chen, G., Lu, J., Lin, F., et al. (2000). Cytochrome c release and apoptosis induced by mitochondrial targeting of nuclear orphan receptor TR3. *Science* **289**, 1159–1164.
- Li, N., Banin, S., Ouyang, H., Li, G.C., Courtois, G., Shiloh, Y., Karin, M., and Rotman, G. (2001). ATM is required for I $\kappa$ B kinase (IKK) activation in response to DNA double strand breaks. *J. Biol. Chem.* **276**, 8898–8903.
- Mahajan, R., Delphin, C., Guan, T., Gerace, L., and Melchior, F. (1997). A small ubiquitin-related polypeptide involved in targeting RanGAP1 to nuclear pore complex protein RanBP2. *Cell* **88**, 97–107.
- Mahanty, S.K., Wang, Y., Farley, F.W., and Elion, E.A. (1999). Nuclear shuttling of yeast scaffold Ste5 is required for its recruitment to the plasma membrane and activation of the mating MAPK cascade. *Cell* **98**, 501–512.
- Makris, C., Roberts, J.L., and Karin, M. (2002). The carboxyl-terminal region of I $\kappa$ B kinase gamma (IKK $\gamma$ ) is required for full IKK activation. *Mol. Cell. Biol.* **22**, 6573–6581.
- Malek, S., Chen, Y., Huxford, T., and Ghosh, G. (2001). I $\kappa$ B $\beta$ , but not I $\kappa$ B $\alpha$ , functions as a classical cytoplasmic inhibitor of NF- $\kappa$ B dimers by masking both NF- $\kappa$ B nuclear localization sequences in resting cells. *J. Biol. Chem.* **276**, 45225–45235.
- Mao, Y., Sun, M., Desai, S.D., and Liu, L.F. (2000). SUMO-1 conjugation to topoisomerase I: a possible repair response to topoisomerase-mediated DNA damage. *Proc. Natl. Acad. Sci. USA* **97**, 4046–4051.
- Matunis, M.J., Coutavas, E., and Blobel, G. (1996). A novel ubiquitin-like modification modulates the partitioning of the Ran-GTPase-activating protein RanGAP1 between the cytosol and the nuclear pore complex. *J. Cell Biol.* **135**, 1457–1470.
- May, M.J., D'Acquisto, F., Madge, L.A., Glockner, J., Pober, J.S., and Ghosh, S. (2000). Selective inhibition of NF- $\kappa$ B activation by a peptide that blocks the interaction of NEMO with the I $\kappa$ B kinase complex. *Science* **289**, 1550–1554.
- Miyamoto, S., Seufzer, B., and Shumway, S. (1998). Novel I $\kappa$ B $\alpha$  degradation process in WEHI231 murine immature B cells. *Mol. Cell. Biol.* **18**, 19–29.
- Muller, S., Matunis, M.J., and Dejean, A. (1998). Conjugation with the ubiquitin-related modifier SUMO-1 regulates the partitioning of PML within the nucleus. *EMBO J.* **17**, 61–70.
- Muller, S., Hoegge, C., Pyrowolakis, G., and Jentsch, S. (2001). SUMO, ubiquitin's mysterious cousin. *Nat. Rev. Mol. Cell Biol.* **2**, 202–210.
- Orth, K., Xu, Z., Mudgett, M.B., Bao, Z.Q., Palmer, L.E., Bliska, J.B., Mangel, W.F., Staskawicz, B., and Dixon, J.E. (2000). Disruption of signaling by Yersinia effector YopJ, a ubiquitin-like protein protease. *Science* **290**, 1594–1597.
- Pickart, C.M. (2001). Mechanisms underlying ubiquitination. *Annu. Rev. Biochem.* **70**, 503–533.
- Rodriguez, M.S., Desterro, J.M., Lain, S., Midgley, C.A., Lane, D.P., and Hay, R.T. (1999). SUMO-1 modification activates the transcriptional response of p53. *EMBO J.* **18**, 6455–6461.
- Rodriguez, M.S., Dargemont, C., and Hay, R.T. (2001). SUMO-1 conjugation in vivo requires both a consensus modification motif and nuclear targeting. *J. Biol. Chem.* **276**, 12654–12659.
- Ross, S., Best, J.L., Zon, L.I., and Gill, G. (2002). SUMO-1 modification represses Sp3 transcriptional activation and modulates its subnuclear localization. *Mol. Cell* **10**, 831–842.
- Rui, H.L., Fan, E., Zhou, H.M., Xu, Z., Zhang, Y., and Lin, S.C. (2002). SUMO-1 modification of the C-terminal KVEKVD of Axin is required for JNK activation but has no effect on Wnt signaling. *J. Biol. Chem.* **277**, 42981–42986.
- Salghetti, S.E., Caudy, A.A., Chenoweth, J.G., and Tansey, W.P. (2001). Regulation of transcriptional activation domain function by ubiquitin. *Science* **293**, 1651–1653.
- Seeler, J.S., and Dejean, A. (2003). Nuclear and unclear functions of SUMO. *Nat. Rev. Mol. Cell Biol.* **4**, 690–699.
- Smahi, A., Courtois, G., Vabres, P., Yamaoka, S., Heuertz, S., Munnich, A., Israel, A., Heiss, N.S., Klauck, S.M., Kioschis, P., et al. (2000). Genomic rearrangement in NEMO impairs NF- $\kappa$ B activation and is a cause of incontinentia pigmenti. The International Incontinentia Pigmenti (IP) Consortium. *Nature* **405**, 466–472.
- Sun, S.C., and Ballard, D.W. (1999). Persistent activation of NF- $\kappa$ B by the tax transforming protein of HTLV-1: hijacking cellular I $\kappa$ B kinases. *Oncogene* **18**, 6948–6958.
- Tam, W.F., and Sen, R. (2001). I $\kappa$ B family members function by different mechanisms. *J. Biol. Chem.* **276**, 7701–7704.
- Tibbetts, R.S., Cortez, D., Brumbaugh, K.M., Scully, R., Livingston, D., Elledge, S.J., and Abraham, R.T. (2000). Functional interactions between BRCA1 and the checkpoint kinase ATR during genotoxic stress. *Genes Dev.* **14**, 2989–3002.
- Trompouki, E., Hatzivassiliou, E., Tschirtzlis, T., Farmer, H., Ashworth, A., and Mosialos, G. (2003). CYLD is a deubiquitinating enzyme that negatively regulates NF- $\kappa$ B activation by TNFR family members. *Nature* **424**, 793–796.
- Wang, C., Deng, L., Hong, M., Akkaraju, G.R., Inoue, J., and Chen, Z.J. (2001). TAK1 is a ubiquitin-dependent kinase of MKK and IKK. *Nature* **412**, 346–351.
- Weil, R., Schwamborn, K., Alcover, A., Bessia, C., Di Bartolo, V., and Israel, A. (2003). Induction of the NF- $\kappa$ B cascade by recruitment of the scaffold molecule NEMO to the T-cell receptor. *Immunity* **18**, 13–26.
- Yamamoto, Y., Verma, U.N., Prajapati, S., Kwak, Y.T., and Gaynor, R.B. (2003). Histone H3 phosphorylation by IKK $\alpha$  is critical for cytokine-induced gene expression. *Nature* **423**, 655–659.
- Zhou, B.B., and Elledge, S.J. (2000). The DNA damage response: putting checkpoints in perspective. *Nature* **408**, 433–439.